

A Quantum-Driven Evolutionary Framework for Solving High-Dimensional Sharpe Ratio Portfolio Optimization

Mingyang Yu*

Jiaqi Zhang*

1120240312@mail.nankai.edu.cn
2120250616@mail.nankai.edu.cn

Nankai University
Tianjin, China

Haorui Yang

Nankai University
Tianjin, China

2120240645@mail.nankai.edu.cn

Adam Slowik

Koszalin University of Technology
Koszalin, Poland
adam.slowik@tu.koszalin.pl

Huiling Chen
Wenzhou University
Wenzhou, China
chenhuiling.jlu@gmail.com

Jing Xu
Nankai University
Tianjin, China
xujing@nankai.edu.cn

Abstract

High-dimensional portfolio optimization faces significant computational challenges under complex constraints, with traditional optimization methods struggling to balance convergence speed and global exploration capability. To address this, firstly, we introduce an enhanced Sharpe ratio-based model that incorporates all constraints into the objective function using adaptive penalty terms, transforming the original constrained problem into an unconstrained single-objective formulation. This approach preserves financial interpretability while simplifying algorithmic implementation. To efficiently solve the resulting high-dimensional optimization problem, we propose a Quantum Hybrid Differential Evolution (QHDE) algorithm, which integrates Quantum-inspired probabilistic behavior into the standard DE framework. QHDE employs a Schrödinger-inspired probabilistic mechanism for population evolution, enabling more flexible and diversified solution updates. To further enhance performance, a good point set–chaos reverse learning strategy is adopted to generate a well-dispersed initial population, and a dynamic elite pool combined with Cauchy–Gaussian hybrid perturbations strengthens global exploration and mitigates premature convergence. Experimental validation on CEC benchmarks and real-world portfolios involving 20 to 80 assets demonstrates that QHDE’s performance improves by up to 73.4%. It attains faster convergence, higher solution precision, and greater robustness than seven state-of-the-art counterparts, thereby confirming its suitability for complex, high-dimensional portfolio optimization and advancing quantum-inspired evolutionary research in computational finance.

CCS Concepts

• Computing methodologies → Discrete space search.

Keywords

Portfolio optimization, Differential Evolution, Sharpe ratio-based portfolio, Quantum evolution strategy, Dynamic elite pool

1 Introduction

In finance, a portfolio represents a collection of stocks or assets managed by individuals or institutions. Portfolio optimization entails distributing a fixed budget among the assets to minimize risk while maximizing expected returns. The Modern Portfolio Theory (MPT) employs the mean-variance model to describe the relationship between risk and return [16]. The core principle of this theory quantifies risk using variance, where lower-risk portfolios are typically characterized by smaller variances. However, MPT overlooks practical market constraints and the influence of background risks, such as base requirements, upper and lower bounds, and challenges inherent in managing large-scale asset portfolios [9, 17, 24]. Therefore, real-world portfolio optimization must incorporate these constraints and uncertainties to account for actual market conditions.

Differential Evolution (DE) [5] is a widely used metaheuristic algorithm for global optimization, renowned for its high performance and ease of implementation in various optimization tasks. DE has the advantages of being simple to implement, requiring fewer parameters, and possessing strong global search capabilities, widely adopted in various engineering optimization and scientific research tasks [11, 22, 23, 26, 27]. Given the hybrid decision-making nature of discrete asset selection and continuous weight allocation in portfolio optimization, the real-valued encoding mechanism of DE facilitates a precise characterization of the continuous search space of asset weights, and combined with specialized mapping strategies to effectively handle complex constraints and multi-objective optimization, thereby adapting to both nonlinear and multi-modal requirements in financial decision-making. However, when confronted with high-dimensional complex portfolio problems, DE faces notable limitations. First, it is prone to becoming trapped in local optima, hindering the search for the global optimum. Second, as the dimensionality increases, the search efficiency declines and convergence slows. These limitations restrict the application effectiveness of DE in the field of portfolio optimization. In response to these challenges, the introduction of quantum computing offers a new breakthrough for improving metaheuristic algorithms.

*Both authors contributed equally to this research.

In recent years, quantum computing has emerged as a transformative computational technology, demonstrating significant potential [3, 6]. Quantum computing can exponentially accelerate certain computational tasks through properties such as superposition and entanglement of quantum bits [13, 15]. This acceleration capability confers a distinct advantage in addressing high-dimensional optimization problems with large solution spaces, especially in financial applications such as portfolio optimization, risk assessment, and derivative pricing [14]. In this context, quantum algorithms provide a new perspective on optimization problems, and numerous metaheuristic algorithms based on quantum computing have emerged [2, 4, 20, 21, 28]. Integrating quantum computing with existing optimization approaches can fully harness its global search potential, thereby mitigating the limitations of traditional algorithms under high-dimensional and complex constraints.

In this paper, by combining the strengths and limitations of DE in portfolio optimization with the characteristics of quantum computing, we propose a variant of the DE based quantum theory, referred to as the Quantum Hybrid Differential Evolution Algorithm (QHDE). QHDE incorporates multiple innovative improvements relative to conventional DE. Guided by quantum theory for global search, it more effectively explores optimal portfolio configurations in high-dimensional spaces and converges faster to the global optimum. Furthermore, the incorporation of chaotic reverse learning extends the coverage of initial solutions, resulting in a more advantageous search starting point. Meanwhile, the dynamic elite pool and Cauchy-Gaussian mixed disturbance strategy effectively prevent premature convergence and increase the diversity of the solutions. The combination of these improvement strategies enables QHDE to surpass traditional DE and other metaheuristic algorithms in portfolio optimization, allowing for faster identification of the optimal solution that balances risk and return. The main contributions of this paper are as follows:

(1) Incorporating quantum behavior and probability collapse mechanisms, we design a quantum evolution strategy based on population information exchange, which significantly enhances the algorithm's global search capability and convergence speed.

(2) We introduce an innovative initialization mechanism that combines the good point set method with chaotic reverse learning. This mechanism enhances the quality of initial solutions and improves algorithmic stability, offering a more efficient starting point for subsequent optimization.

(3) We propose a dynamic elite pool strategy and applies Cauchy-Gaussian random perturbation. This strategy mitigates premature convergence to local optima, enhances solution diversity, and strengthens global search capability.

(4) We apply QHDE to portfolio optimization, where it outperforms seven state-of-the-art algorithms, exceeding the runner-up by up to 73.4%. This approach significantly accelerates convergence while enhancing accuracy, proving to be an efficient and robust solution for high-dimensional problems.

The structure of this paper is as follows: In Section 2, we discuss various modeling approaches for portfolio selection problem and analyze their advantages and disadvantages. In Section 3, we provide a detailed discussion of the original DE algorithm and the improvements proposed in this paper. In Section 4, we evaluate and analyze

the performance of QHDE through relevant experiments, and apply the algorithm to solve a portfolio selection problem involving multiple stocks. Finally, we conclude the paper and discusses future research directions in Section 5.

2 Math Equations

This section primarily introduces modeling methods of the portfolio selection problem, laying the foundation for the subsequent introduction of optimization techniques.

2.1 Mean-Variance Model

The Mean-Variance Model serves as a foundational mathematical framework for portfolio optimization. In this model, the objective function focuses on minimizing the portfolio's overall risk, while the expected mean return is incorporated as a constraint. This ensures the portfolio achieves the desired return level while maintaining minimal risk. Its mathematical form is expressed as follows:

$$\min \sum_{i=1}^M \sum_{j=1}^M E_i E_j Q_{ij} \quad (1)$$

$$\text{s.t. } \sum_{i=1}^M E_i \alpha_i = R \quad (2)$$

$$\sum_{i=1}^M E_i = 1 \quad (3)$$

$$0 \leq E_i \leq 1, \quad i = 1, 2, \dots, M \quad (4)$$

Equation (1) defines the objective function for minimizing portfolio risk. Here, M denotes the total number of stocks, E_i and E_j represents the investment weight of the i th and j th stock respectively, Q_{ij} signifies the covariance between the i th and j th stocks, and α_i denotes the expected return of the i th stock. This function aims to minimize the portfolio's overall risk by optimizing the allocation of weights across the assets. Equation (2) ensures that the total return of the investment portfolio reaches the predetermined expected return R . Equation (3) stipulates that the sum of the investment weights for all stocks must equal 1 to guarantee the complete allocation of funds. Equation (4) further limits each investment weight between 0 and 1, which ensures that no short-selling is allowed.

2.2 Efficient Frontier

In portfolio selection problems, investors are required to construct a portfolio that maximizes expected returns while minimizing risk. Unlike the mean-variance model, which treats expected returns as a constraint, the efficient frontier model directly incorporates expected returns into the objective function as one of the key components of optimization. Specifically, the objective function balances the trade-off between risk and return by introducing a penalty term for the return, and the expression is:

$$\min \left[\omega \left(\sum_{i=1}^M \sum_{j=1}^M E_i E_j Q_{ij} \right) - (1 - \omega) \left(\sum_{i=1}^M E_i \alpha_i \right) \right] \quad (5)$$

$$\text{s.t. } \sum_{i=1}^M E_i = 1 \quad (6)$$

$$0 \leq E_i \leq 1, \quad i = 1, 2, \dots, M \quad (7)$$

where $\omega \in [0, 1]$, and the two constraints in Equation (6) and (7) are consistent with the mean-variance model, ensuring full allocation of funds and non-negativity constraints.

2.3 Sharpe Ratio Model

In the Sharpe Ratio Model, the focus shifts from analyzing these two parameters separately to considering their ratio. The Sharpe ratio measures the excess return per unit of risk and serves as an important indicator that comprehensively reflects the balance between portfolio return and risk. Its mathematical expression is as follows:

$$\text{Sharpe - ratio} = \frac{R_p - R}{\text{std}(p)} \quad (8)$$

where p denotes a portfolio, R_p is the return of the portfolio, and R is the risk-free rate of return. $\text{std}(p)$ represents the standard deviation of the portfolio, which can be considered as the risk of portfolio. By specifying R_p and $\text{std}(p)$ in Equation (8) and integrating the previously mentioned constraints, the complete optimization model is given as:

$$\max \frac{\sum_{i=1}^M E_i \alpha_i - R}{\sqrt{\sum_{i=1}^M \sum_{j=1}^M E_i E_j Q_{ij}}} \quad (9)$$

$$\text{s.t.} \quad \sum_{i=1}^M E_i = 1 \quad (10)$$

$$0 \leq E_i \leq 1, \quad i = 1, 2, \dots, M \quad (11)$$

2.4 Our unconstrained model

In this study, we refer to the Sharpe ratio model and reference [9] to transform the original constrained optimization model into an unconstrained single-objective optimization problem. The transformed objective function is:

$$F(E) = \max \beta_1 \left[\frac{\sum_{i=1}^M E_i \alpha_i - R}{\sqrt{\sum_{i=1}^M \sum_{j=1}^M E_i E_j Q_{ij}}} \right] - \beta_2 \left(\sum_{i=1}^M E_i - 1 \right)^2 - \beta_3 (E_i - 1 \geq 0) (E_i - 1) - \beta_4 (-E_i \geq 0) (-E_i) \quad (12)$$

where $\left(\sum_{i=1}^M E_i - 1 \right)^2$ represents the equality constraint specified in Equation (10), ensuring the sum of the investment weights equals 1. While $(E_i - 1 \geq 0) (E_i - 1)$ and $(-E_i \geq 0) (-E_i)$ correspond to the inequality constraints outlined in Equation (11), which ensure the weights remain within valid bounds. β_1 , β_2 , β_3 , and β_4 denote the penalty weights associated with these constraints.

3 Methodology Overview: original DE and Proposed Improvements

In this section, we will first provide a detailed introduction to the original DE. Subsequently, we will conduct an in-depth study of the proposed QHDE, including a good point set-chaos reverse learning initialization mechanism, a quantum evolution strategy based on population information exchange, and a dynamic elite pool and Cauchy-Gaussian mixed disturbance strategy.

3.1 The original DE

DE is a classic population-based intelligent optimization algorithm, widely used in global optimization problems in continuous spaces. Its core consists of four operations: initialization, mutation, crossover, and selection. In each generation t , for individual $x_r(t)$, the mutation vector is generated as:

$$v_i(t+1) = x_{r_1}(t) + F \cdot (x_{r_2}(t) - x_{r_3}(t)) \quad (13)$$

where x_{r_1} , x_{r_2} and x_{r_3} denote different individuals randomly selected from the population; F represents the mutation parameter, typically taking values in the range $[0, 2]$; and t represents the iteration count. Subsequently, a binomial crossover operation is employed to generate the trial vector $u_{i,j}$

$$u_{i,j}(t+1) = \begin{cases} v_{i,j}(t+1) & \text{if } \text{rand}_j(0, 1) \leq CR \text{ or } j = j_{\text{rand}} \\ x_{i,j}(t) & \text{otherwise} \end{cases} \quad (14)$$

where $u_{i,j}$ represents the j th component of the trial vector u_i , $\text{rand}_j(0, 1)$ represents a random number in the range $[0, 1]$, CR denotes the crossover probability, and j_{rand} denotes a randomly selected index to ensure that u_i has at least one component from v_i . Finally, if the fitness of the test individual is superior to that of the original individual, it will enter the next generation:

$$x_i(t+1) = \begin{cases} u_i(t+1) & \text{if } f(u_i(t+1)) \leq f(x_i(t)) \\ x_i(t) & \text{otherwise} \end{cases} \quad (15)$$

where $f(x)$ denotes the fitness value of individual x .

3.2 Our proposed QHDE

The portfolio optimization involves multiple variables and complex constraints, requiring algorithms to efficiently explore large-scale search spaces. Therefore, the goal of the improvements is to enhance the algorithm's performance in high-dimensional complex problems, especially in terms of stability and accuracy when dealing with multiple local optima and nonlinear constraints. To achieve this, quantum behavior, adaptive mechanisms and more efficient perturbation strategies are incorporated for strengthening the algorithm's global search capability. These enhancements significantly boost the efficiency of the DE algorithm while mitigating the risk of being trapped in local optima. As a result, the algorithm becomes more robust and better equipped to handle the challenges of complex portfolio optimization problems.

3.2.1 a good point set-chaos reverse learning initialization mechanism. In metaheuristic algorithms, the quality of the initial solution significantly influences the search outcome. Since the random numbers generated by the system are not entirely random, they often exhibit disadvantages such as uneven distribution or tendency to cluster. Hence, to ensure that the values are as uniformly distributed as possible in the search space and to improve the ergodicity of the initial solution, we utilize the good points set to initialize the population. Let G_s represent the unit hypercube in the s -dimensional space. If $r \in G_s$, then the set of points is given as:

$$GP_n(k) = \left(\left\{ r_1^{(n)} \times k \right\}, \dots, \left\{ r_s^{(n)} \times k \right\} \right), \quad 1 \leq k \leq n \quad (16)$$

If the deviation satisfies $\varphi(n) = C(r, \varepsilon) n^{-1+\varepsilon}$, where $C(r, \varepsilon)$ represents a constant that depends only on r and ε , $GP_n(k)$ is referred

to as the good point set. Let $r = \{2 \cos(2\pi i/pn), 1 \leq i \leq s\}$, where pn represents the smallest prime number satisfying $(p-3)/2 \geq s$, and r represents termed a good point. After generating the good point set, it is mapped to the search space as:

$$X_{i,j} = (ub - lb) \times \{GP_n(k)\} + lb \quad (17)$$

where X represents the initial solution, $X_{i,j}$ denotes the j th component of the i th individual, and ub and lb respectively represent the upper and lower bounds of the search space.

Reverse learning is a perturbation mechanism, whose fundamental principle lies in obtaining the reverse solution of a known solution in the target space through reverse learning, and then choosing a superior solution from them as the current solution. Chaotic systems are a kind of nonlinear and highly sensitive deterministic systems. Although their behaviors do not exhibit periodicity or tend toward a stable state, they always maintain certain boundaries. The inherent regularity and randomness of chaotic systems, along with their ergodicity and unpredictability, make them a reliable source of randomness, offering more effective search strategies for heuristic optimization algorithms compared to traditional random sequences. In this paper, we adopt the Logistic chaotic mapping to initialize the population X generated by the optimal point set:

$$G^{t+1} = \mu \times G^t (1 - G^t) \quad (18)$$

where, μ represents the chaotic coefficient, $\mu \in (2, 4)$, and G represents the chaotic factor generated by the Logistic chaotic mapping. The initialization process combines the Logistic chaotic mapping and reverse learning as follows:

$$X' = G \times (ub - lb) - X \quad (19)$$

where X' denotes the solution adjusted through reverse learning. After merging X' and X , N individuals with the top one-half fitness values are selected as the new population.

3.2.2 quantum evolution strategy based on population information exchange. Traditional DE often encounters issues like slow convergence and a propensity to become stuck in local optima, particularly when addressing complex optimization problems like portfolio optimization. To address these challenges, this paper proposes integrating quantum theory into the DE framework. The quantum search mechanism simulates the process in which particles in a potential field move towards the lowest potential energy point in quantum mechanics. Specifically, the search space is considered as a potential field in quantum mechanics, the global optimum solution corresponding to the lowest point of the potential energy in the field, and the optimization process is the movement of particles towards this lowest potential energy point in this potential field. In quantum mechanics, the dynamic behavior of particles is described by the Schrödinger equation:

$$j\hbar \frac{\partial}{\partial \tau} \Psi(q, \tau) = \left(-\frac{\hbar^2}{2m} \nabla^2 + V(q) \right) \Psi(q, \tau) \quad (20)$$

where \hbar represents the Planck constant, wave function $\Psi(q, \tau)$ represents the probability density of a particle being at position q at time τ , m represents the mass of the particle, ∇^2 represents the Laplacian operator, which represents the spatial distribution of the wave function, and $V(q)$ denotes the potential energy distribution

function. The potential energy distribution of the Delta potential well is:

$$V(q) = -\gamma \delta(q) \quad (21)$$

where γ represents the depth of the potential well, and $\delta(q)$ denotes the Dirac delta function. The particle's wave function is:

$$\Psi(q) = \frac{1}{\sqrt{L}} e^{-|q|/L} \quad (22)$$

where L represents the characteristic length parameter of the potential well, which controls the decay rate of the wave function. The probability density function is given by:

$$H(y) = |\Psi(y)|^2 = \frac{1}{\sqrt{L}} e^{-2|q|/L} \quad (23)$$

We use the Monte Carlo method to measure the position by collapsing the quantum state to a classical state:

$$y = \pm \frac{L}{2} \ln \left(\frac{1}{r_4} \right) \quad (24)$$

where r_4 represents a random variable in $[0, 1]$. Based on the above quantum theory, we propose a Quantum Evolution Strategy based on Population Information Exchange. The core idea of this strategy is to enhance the global search capability of the optimization algorithm by introducing a population information exchange mechanism and combining the characteristics of quantum evolution. First, the position of the population's centroid is defined as:

$$x_{\text{mean}} = \frac{1}{N} \sum_{i=1}^N x_i \quad (25)$$

The adaptive factor is defined as:

$$\eta = (w_2 - w_1) \times \frac{T_{\text{max}} - t}{T_{\text{max}}} + w_1 \quad (26)$$

where w_1 and w_2 denote control factors that determine the adjustment range of the adaptive factor, T_{max} represents the maximum number of iterations, and t denotes the current iteration count. The parameter expressions are:

$$d = x_i + (c_1 \times r_5 \times (x_i - x_{\text{worse}})) + (c_2 \times (1 - r_5) \times (x_{\text{best}} - x_i)) \quad (27)$$

$$b = \frac{\eta}{2} \times |x_i - x_{\text{best}}| \quad (28)$$

$$z = \log \left(\frac{1}{r_6} \right) \quad (29)$$

where d represents the individual's position update direction, influenced by the current individual position x_i , the positions of the worst individual with the highest value of objective function x_{worse} and the best individual with the smallest value of objective function x_{best} ; c_1 and c_2 denote the information exchange factors that control the degree of the individual's response to the worst and best individual positions; b represents the individual's step size, which is adjusted based on the adaptive factor and the distance between the individual and the best individual in the population; v represents quantum perturbation, which influences the individual's position update; r_5 and r_6 denote random numbers between $[0, 1]$. The update direction of the individual's position is determined probabilistically:

$$x_{\text{new}} = \begin{cases} d + b \times z, & \text{if rand} < 0.5 \\ d - b \times z, & \text{otherwise} \end{cases} \quad (30)$$

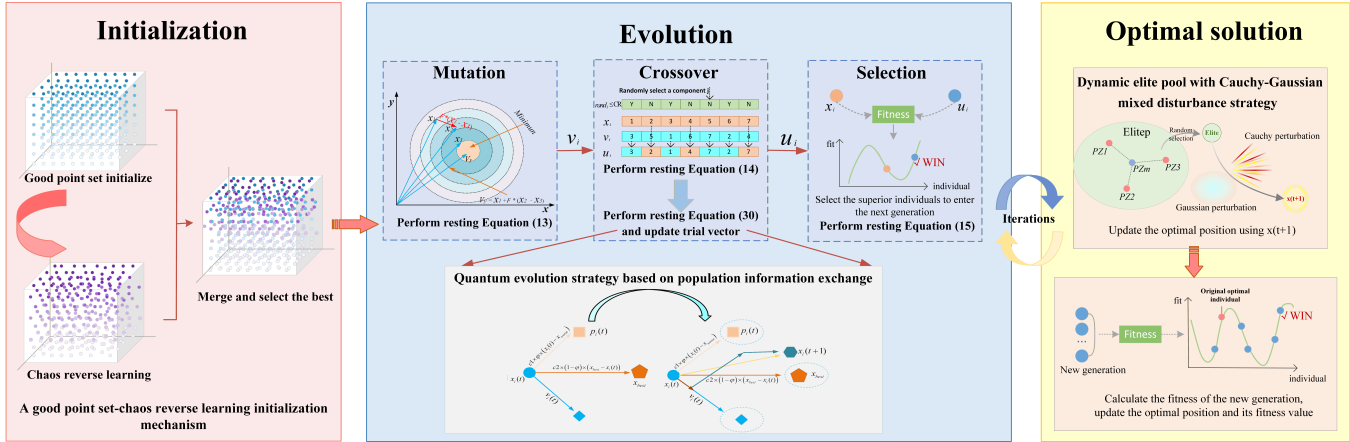


Figure 1: Flow chart of QHDE

3.2.3 dynamic elite pool with Cauchy-Gaussian mixed disturbance strategy. In the later iterations of the DE, population individuals often tend to cluster around the current best solution due to rapid assimilation. If the current solution is not globally optimal, the population may prematurely fall into a local optimum, leading to a stagnation of the search. To address this issue, this paper proposes a dynamic elite pool and Cauchy-Gaussian mixed disturbance strategy. This strategy enhances the algorithm's global search ability and diversity of solutions by constructing an elite pool (*Elitep*) consisting of the top-performing individuals, thereby avoiding the algorithm from being trapped in local optima. The specific procedure is as follows:

First, based on the fitness evaluations of the population, the three highest fitness individuals, denoted as *PZ1*, *PZ2*, and *PZ3*, are selected. Then the arithmetic mean of their positions is calculated to obtain the average position *PZm*:

$$PZm = \frac{(PZ1 + PZ2 + PZ3)}{3} \quad (31)$$

Next, these three top individuals, along with their average position, are included in *Elitep*. During each iteration, a position is randomly selected from *Elitep* as a reference point to guide the movement direction of individuals.

Cauchy-Gaussian mutation is a hybrid mutation method that combines the long-tail characteristics of the Cauchy distribution with the concentration tendency of the Gaussian distribution. The purpose of this strategy is to apply strategic random perturbations to the global best individual, exploring potentially unknown beneficial regions around the global optimum, while maintaining the "memory" of the current best solution. After combining the dynamic elite pool and Cauchy-Gaussian perturbation strategies, the update formula for the new individual's position is as follows:

$$x_{\text{best}}^{t+1} = \text{Elite} \times [\rho \times \text{Cauchy}(0, 1) + (1 - \rho) \times \text{Gauss}(0, 1)] \quad (32)$$

where x_{best}^{t+1} represents the global best individual in the $(t+1)$ generation. ρ denotes a weight coefficient that balances the contributions of the Cauchy distributions and Gaussian distributions in the mutation operation, with values ranging from $[0, 1]$. The choice of this parameter affects the randomness and distribution of the mutation.

Cauchy($0, 1$), with its long tails, introduces large perturbations that help escape local optima and enhance global search. In contrast, Gauss($0, 1$) concentrates around the mean, enabling stable, fine-grained local search. The parameter ρ balances the influence of these two distributions, allowing the mutation to adjust between global exploration and local exploitation.

In summary, the pseudocode and workflow of the QHDE is presented in Algorithm 1 and Figure 1.

3.3 Time and space complexity analysis

The computational complexity of QHDE mainly depends on population initialization and core operations such as fitness evaluation and iterative updates. With population size N , iteration limit T_{max} , and dimension D , the original complexity is $O(T_{\text{max}}ND)$. The improved QHDE introduces good-point-set chaos-reverse initialization, quantum evolution with information exchange, and a dynamic elite pool with Cauchy-Gaussian disturbance. Initialization operations (good-point-set generation, chaotic mapping, and reverse learning) each cost $O(ND)$ and are executed once. Quantum evolution updates and the elite-pool disturbance strategy both require $O(ND)$ per iteration, giving $O(T_{\text{max}}ND)$. Thus, the total complexity remains $O(T_{\text{max}}ND)$, consistent with the original algorithm.

The space complexity of DE depends on storing the population, fitness values, and candidate solutions. With population size N and dimension D , storing positions and temporary candidates requires $O(ND)$, while fitness values need $O(N)$. Thus, the overall complexity is $O(ND)$. In the improved QHDE, storing good-point sets, reverse individuals, quantum states, and the elite pool also requires $O(ND)$, so the total space complexity remains $O(ND)$.

4 Experiments and comprehensive analysis

This section provides a detailed discussion of the experimental results obtained by applying QHDE to numerical optimization tasks and portfolio selection problems. Firstly, we conduct numerical optimization tests using the CEC 2020 and CEC 2022 test suite to preliminarily evaluate the performance of the algorithm in optimizing multimodal functions and high-dimensional problems. Next, we apply QHDE to four portfolio selection problems (involving 20, 40,

Algorithm 1 Quantum Hybrid Differential Evolution (QHDE)

```

1: Initialize Problem Setting (dimension ( $D$ ),  $ub$ ,  $lb$ , population
   ( $N$ ), iterations ( $T_{\max}$ ))
2: Create an initial population  $X = (x_1, x_2, \dots, x_N)$ ,  $x_i \in D$  using
   (16), (17)
3: Generate the population  $X'$  using (18), (19)
4: Merge  $X'$  with  $X$ , and select  $N$  individuals with the highest
   fitness values as the new population  $P$ 
5: while  $t \leq T_{\max}$  do
6:   for  $i = 1$  to  $N$  do
7:     Randomly select  $x_{r_1}, x_{r_2}, x_{r_3}$  from the population and
       calculate  $v_i$  using (13)
8:     Generate trial vector  $u_i$  using (14)
9:     Generate  $x_{new}$  using (30)
10:    if  $X_i$  surpasses  $u_i$  then
11:       $u_i = x_{new}$ 
12:    end if
13:    if  $f(u_i) \leq f(x_i)$  then
14:      Insert  $u_i$  into new generation  $P_{new}$ 
15:    else
16:      Insert  $x_i$  into new generation  $P_{new}$ 
17:    end if
18:  end for
19:  Select the fittest individuals  $PZ1, PZ2, PZ3$  and calculate
    $PZm$  using (31) to form the elite pool
20:  Generate  $x_{best}^{t+1}$  using (32)
21:  if  $x_{best}^{t+1}$  surpasses  $pos_{best}$  then
22:     $pos_{best} = x_{best}^{t+1}$ 
23:  end if
24:  Update best global position  $pos_{best}$  and its fitness value
    $fit_{best}$ 
25:   $P = P_{new}$ 
26:   $t = t + 1$ 
27: end while
28: return  $pos_{best}$  and  $fit_{best}$ 

```

60, and 80 stocks, respectively) and compare its performance with seven metaheuristic algorithms that are widely employed in this field to validate the superiority of QHDE in portfolio optimization. The simulations were conducted on a Windows 11 platform with a 64-bit operating system. The analyses were carried out using MATLAB 2023b on a system powered by an AMD Ryzen 7 4800H CPU at 2.30 GHz and 16 GB of RAM.

4.1 Test functions and comparison algorithms

To initially assess the performance of the proposed QHDE, we utilized the CEC 2020 test suite [12] and CEC 2022 [18], which contain diverse, high-dimensional, constrained, and multimodal optimization problems closely mirroring real portfolio-optimization challenges. Their emphasis on non-convex objectives, multiple local optima, and complex constraints makes them strong proxies for balancing return-risk trade-offs. These benchmarks therefore provide a rigorous and representative basis for assessing QHDE's effectiveness.

Table 1: Parameter configurations for competing algorithms

Algorithm	Parameter	Value
SASS	$NP_{min}, H, P_{gr}, \sigma$	4, 5, 0.2, 0.1
COLSHADE	H, r, p, α	5, 2.6, 0.11, 1.5
sCMAES	σ	0.3
HSEPSO	w, c	[0.4, 0.95], [1.2, 2]
NDSOT	$TOL, MAX-INC, w, c_3, c_4$	$10^{-6}, 10, 0.5, 1.0, 1.0$
DE	β, P_c	0.5, 0.5
ADE	β, P_c	[0.2, 0.8], 0.5
QHDE	$\beta, P_c, w_1, w_2, c_1, c_2$	0.5, 0.1, 0.5, 1, 1.5, 1.5

The performance of QHDE was systematically compared against seven well-known algorithms. These are categorized into two distinct groups for a structured analysis:

State-of-the-art algorithm: Self-adaptive spherical search algorithm [10] (SASS), L-SHADE for Constrained Optimization with Levy Flights [8] (COLSHADE), Simple Modification in Covariance Matrix Adaptation Evolution Strategy [19] (sCMAES), Hierarchical Self Evolutionary PSO [25] (HSEPSO), Niching Swarm Dynamic Optimization with TCMAES [7] (NDSOT).

DE and its improved variants: This includes the original Differential Evolution algorithm [5] (DE), the Advanced Differential Evolution [1] (ADE).

Table 1 provides an overview of the parameter settings for eight different MH algorithms.

4.2 Quantitative evaluation

This section provides a comprehensive evaluation of the QHDE's performance using the CEC 2020 and CEC 2022 test suite. To ensure consistency, the experimental parameters were standardized with a population size of 30 and a maximum of 500 iterations, and each algorithm was executed 30 independent runs.

To better illustrate the performance of each algorithm, we summarize the ranking distribution of each algorithm, as shown in Figure 2. In the 10-dimensional benchmarks, QHDE achieved the best performance on two functions, ranked second on four, and third on two. Consequently, it consistently placed within the top three in 80% of the test instances, and didn't exhibit the worst performance on any problem, demonstrating exceptional competitiveness and optimization precision. In contrast, although SASS and sCMAES secured the top rank in slightly more instances (one additional count), they exhibited significant performance volatility, with over half of their rankings classified as 'Other' or lower. Notably, while the rankings of the original DE were predominantly concentrated below the third position, QHDE successfully elevated its standing to the first and second tiers. This substantial improvement substantiates that the incorporated quantum evolutionary strategy effectively enhances the algorithm's capability to escape local optima and accelerates convergence. Overall, QHDE delivers not only high-quality solutions but also exceptional stability across different functions, proving to be the most robust algorithm in this comparative study.

Figure 3 presents the Friedman rank radar plot of all participating algorithms on the CEC 2022 benchmark suite. As evident in

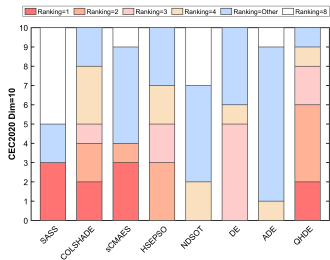


Figure 2: Ranking distribution of different algorithms on CEC 2020 (Dim=10).

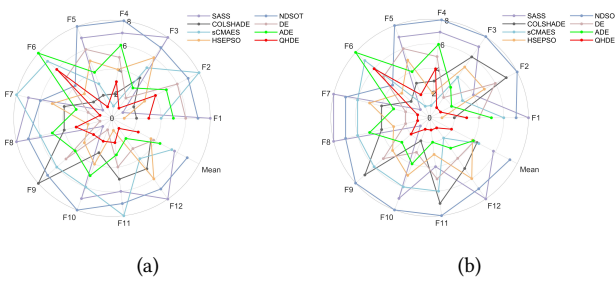


Figure 3: Ranking distribution of different algorithms on CEC 2022. (a) Dim = 10, (b) Dim = 20.

Figure 3(a), QHDE (in red) consistently achieves lower rankings across the majority of test functions, forming a compact shape near the center of the plot. With the increase in dimensionality, the superiority of QHDE becomes even more pronounced. In Figure 3(b), its compactness is further accentuated as the curve closely hugs the central region, indicating that QHDE maintains top-tier performance across diverse problem types with minimal volatility. Notably, QHDE ranks first on functions F2, F3, F7, F8, F10, F11, and F12, which are known for their high complexity and multimodality. The overall rank of QHDE is the lowest among all contenders, further confirming its superior and robust optimization capability across a wide range of scenarios.

As clearly shown in Figure 4, the boxplot analysis of various algorithms on representative functions reveals a significant stability advantage of QHDE. The box of the QHDE boxplot is relatively narrow, indicating a highly concentrated data distribution. This suggests that, across multiple experimental runs, the results generated by QHDE exhibit minimal dispersion, and the search process remains stable. For instance, when dealing with different types of CEC 2020 functions, regardless of the complexity and dimensionality of the functions, QHDE can precisely adjust its search direction and strategy by virtue of its three embedded improvement mechanisms, avoid getting trapped in local optima, thereby continuously and stably output high-quality solutions. In contrast, for algorithms such as SASS, COLSHADE, HSEPSO and NDSOT, the overall positions of the boxplots are relatively higher. This suggests that their results are relatively suboptimal and that their robustness is weaker.

More performance details (such as the average values, standard deviations, Friedman means, etc.) are provided in the appendix.

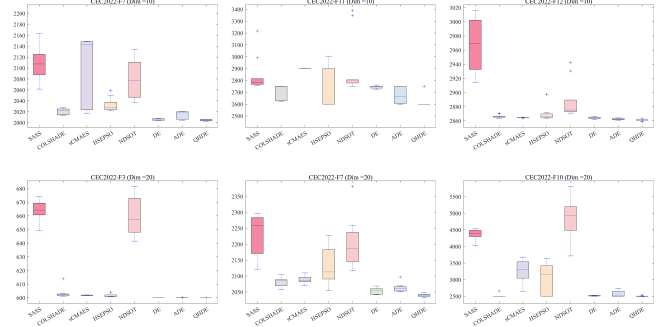


Figure 4: Box plots of QHDE and other algorithms on CEC 2022 functions.

4.3 Portfolio selection

In this section, QHDE was applied to four portfolio selection problems to verify its superiority in portfolio optimization. All the stock data used in the experiments are derived from the CSI 300 Index jointly released by the Shanghai Stock Exchange and the Shenzhen Stock Exchange. The experimental data comprised the closing prices of these stocks from October 8, 2024, to November 13, 2024. We conducted a preliminary analysis of these stock data and selected the best 20, 40, 60, and 80 stocks from the 300 stocks respectively based on the average daily return during this period to form four portfolio selection problems. To eliminate bias, all eight algorithms were provided with the same computational basis, with a population size of 50 and 100 iterations. We evaluated the performance of these algorithms using three key metrics: the objective function $F(E)$ in Equation (12), the Sharpe ratio (S_r) in Equation (8), and the equality constraint $S(E)$ in Equation (10). The results are shown in Table 2, where the best-performing algorithm among the eight comparison algorithms is highlighted in bold.

The results presented in Table 2 indicate that, across four portfolio optimization tasks of different scales, QHDE consistently exhibits remarkable and stable comprehensive performance. The $F(E)$ values of QHDE in the four portfolios are 26.66, 22.89, 16.83, and 7.53, representing the highest scores for each respective scale. Notably, QHDE achieves performance gains of 29.5%, 29.6%, 73.4%, and 68.8% over the runner-up, thereby demonstrating its outstanding capability in maximizing returns. Furthermore, the S_r of QHDE consistently surpasses that of other comparative algorithms, indicating its effectiveness in balancing risk and return to achieve superior risk-adjusted returns. It is worth noting that in small-scale tasks, the optimal value obtained by DE ranks second only to QHDE, suggesting that DE possesses a certain degree of exploitation capability in complex portfolio problems. However, as the scale increases, the performance of DE deteriorates rapidly. Specifically, its $S(E)$ value at 60 dimensions is significantly higher than expected, revealing its limitations in handling complex constraints. In contrast, the proposed QHDE maintains values extremely close to 1 across all test scales. It not only improves optimization precision but also

Table 2: Four portfolios' results solved by seven metaheuristic algorithms

Algorithm	20 stacks			40 stacks			60 stacks			80 stacks		
	F(E)	Sr	S(E) ³									
SASS	-1.99E+04	13.25	1.141	-1.65E+06	5.126	2.284	-6.72E+06	2.622	3.593	-1.26E+07	0.974	4.550
COLSHADE	15.39	15.49	1.000	-6.27E+05	2.807	1.792	-1.54E+07	2.461	4.920	-1.12E+08	0.700	11.56
sCMAES	17.63	17.63	1.000	-2.71E+06	4.424	2.647	-2.94E+07	1.355	6.426	-9.33E+07	0.704	10.66
HSEPSO	11.55	11.562	1.000	11.10	11.11	1.000	3.362	3.363	1.000	-6.18E+05	1.896	1.786
NDSOT	4.00E+06	1.699	3.000	6.40E+07	0.852	9.000	1.96E+08	0.573	15.00	4.84E+08	0.467	23.00
DE	20.58	21.04	0.999	10.11	14.718	0.998	-1.76E+06	2.974	2.328	-2.08E+07	1.515	5.555
ADE	19.94	19.96	1.000	17.66	17.80	1.000	9.703	10.50	1.001	4.464	6.644	0.999
QHDE	26.66	26.66	1.000	22.89	23.10	1.001	16.83	16.91	1.000	7.536	7.750	1.000

effectively resolves the deficiencies of DE in constraint handling, thereby exhibiting superior comprehensive performance.

Upon observing Table 2, it can be noted that as the scale of the stock portfolio increases, the Sr gradually decreases. This is associated with a wider range of stock selections. The overall average expected return of 80 stocks is lower than that of the optimal 20-stock portfolio. This phenomenon is consistent with real investment environments, demonstrating the reliability and robustness of the model proposed in this paper.

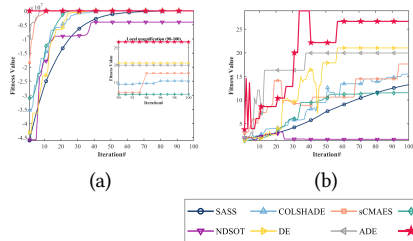


Figure 5: Evaluation and comparison of QHDE applied to 20 stocks alongside other metaheuristic algorithms. (a) illustrates the overall objective function value F(E), (b) presents the Sharpe ratio (Sr), and (c) presents the equality constraint S(E).

To further analyze the performance of the algorithms, Figure 5 presents the iterative process of each algorithm. Constrained by the length of the paper, only the iterative process of 20 stocks is presented in the main text. The convergence details of other scales can be found in the appendix. As shown in Figure 5(a), QHDE achieves the highest F(E) value and converges the fastest, highlighting its significant advantage in global search and convergence efficiency. Other algorithms lagged significantly in both speed and optimization quality. Furthermore, DE achieves final convergence after approximately 50 iterations. Although its optimal value ranks second only to QHDE, its overall performance is markedly inferior. This reaffirms that DE's limited convergence speed hampers its exploitation potential in complex portfolios. In contrast, by incorporating quantum computing strategies, QHDE significantly accelerates the convergence process and enhances optimization precision.

Figure 5(b) displays the Sr of the algorithms. QHDE still achieves the highest Sr, with a stable convergence process. Although its convergence speed is slightly slower than ADE, its final optimization result significantly outperforms the other algorithms. This indicates that QHDE is capable of consistently providing high returns while controlling risk, demonstrating good risk-return balance.

Figure 5(c) shows the convergence of the equality constraint S(E). QHDE exhibits a significant advantage in handling equality constraints, rapidly approaching 1 during the initial iterations, whereas other competing algorithms require dozens of iterations to approach the feasible region, with some (e.g., SASS, NDSOT) failing to converge entirely. The magnified view further confirms that QHDE maintains an error-free and stable state throughout the entire process, demonstrating its outstanding reliability in complex constraint environments.

In summary, QHDE, as a hybrid optimization algorithm based on quantum evolutionary strategies, demonstrates significant advantages in complex portfolio optimization tasks. It not only significantly improves the algorithm's global exploration and local exploitation capabilities but also exhibits strong adaptability and reliability when facing high-dimensional complex constraint problems. These characteristics make QHDE an effective tool for solving complex financial optimization problems and providing an efficient and precise solution to portfolio selection problems.

5 Conclusion

In this paper, we propose a quantum variant of Differential Evolution, QHDE, and apply it to a classic financial portfolio optimization problem. QHDE integrates three major strategies: (1) a good-point-set–chaos reverse-learning initialization mechanism that increases initial population diversity; (2) a quantum evolution strategy that drives individuals toward low-potential regions based on population information exchange, enhancing global exploration while maintaining diversity through quantum behavior and probabilistic collapse; (3) a dynamic elite pool with Cauchy–Gaussian mixed perturbation that prevents premature convergence by introducing strategic disturbances to elite individuals in later stages. Together, these mechanisms accelerate global convergence and improve robustness in complex search spaces.

The effectiveness of QHDE is demonstrated on the CEC 2020 and CEC 2022 benchmark suites, where it is compared with seven

state-of-the-art optimizers. Statistical results show that QHDE consistently outperforms the competitors. In portfolio optimization experiments, QHDE achieves superior returns, lower risk, and faster convergence, exhibiting strong global exploration and local exploitation capabilities. These advantages position QHDE as a competitive solver for practical financial optimization tasks.

Future research could extend the application of QHDE to other financial optimization challenges, such as multi-objective investment strategies and dynamic portfolio management. Furthermore, comprehensive studies on the key parameters of quantum evolutionary strategies could further refine the algorithm's performance.

Acknowledgments

This work was supported by Natural Science Foundation of Tianjin Municipality (21JCYBJC00110), Tianjin Science and Technology Major Project (24ZXZSSS00420), Major Projects of the National Natural Science Foundation of China (72495155).

References

- [1] Behzad Abbasi, Vahid Majidnezhad, and Seyedali Mirjalili. 2024. ADE: advanced differential evolution. *Neural Computing and Applications* 36, 25 (2024), 15407–15438.
- [2] Sebastian Brandhofer, Daniel Braun, Vanessa Dehn, Gerhard Hellstern, Matthias Hüls, Yanjun Ji, Ilia Polian, Amandeep Singh Bhatia, and Thomas Wellens. 2022. Benchmarking the performance of portfolio optimization with QAOA: S. Brandhofer et al. *Quantum Information Processing* 22, 1 (2022), 25.
- [3] Junwen Chen, Xuemei Qi, Linfeng Chen, Fulong Chen, and Guihua Cheng. 2020. Quantum-inspired ant lion optimized hybrid k-means for cluster analysis and intrusion detection. *Knowledge-Based Systems* 203 (2020), 106167.
- [4] Min-Yuan Cheng and Moh Nur Sholeh. 2025. Artificial satellite search: A new metaheuristic algorithm for optimizing truss structure design and project scheduling. *Applied Mathematical Modelling* 143 (2025), 116008. doi:10.1016/j.apm.2025.116008
- [5] Swagatam Das and Ponnuthurai Nagaratnam Suganthan. 2010. Differential evolution: A survey of the state-of-the-art. *IEEE transactions on evolutionary computation* 15, 1 (2010), 4–31.
- [6] Wu Deng, Shifan Shang, Xing Cai, Huimin Zhao, Yongquan Zhou, Huayue Chen, and Wuquan Deng. 2021. Quantum differential evolution with cooperative coevolution framework and hybrid mutation strategy for large scale optimization. *Knowledge-Based Systems* 224 (2021), 107080.
- [7] Shoei Fujita, Ryuki Ishizawa, Hiroyuki Sato, and Keiki Takadama. 2025. Adaptive Multi-Population Dynamic Optimization for Multimodal Dynamic Function Optimization. In *Proceedings of the Genetic and Evolutionary Computation Conference*. 1540–1548.
- [8] Javier Gurrola-Ramos, Arturo Hernández-Aguirre, and Oscar Dalmau-Cedeño. 2020. COLSHADE for real-world single-objective constrained optimization problems. In *2020 IEEE congress on evolutionary computation (CEC)*. IEEE, 1–8.
- [9] Ameer Tamoor Khan, Xinwei Cao, Shuai Li, Bin Hu, and Vasilios N Katsikis. 2021. Quantum beetle antennae search: a novel technique for the constrained portfolio optimization problem. *Science China Information Sciences* 64, 5 (2021), 152204.
- [10] Abhishek Kumar, Swagatam Das, and Ivan Zelinka. 2020. A self-adaptive spherical search algorithm for real-world constrained optimization problems. In *Proceedings of the 2020 Genetic and Evolutionary Computation Conference Companion*. 13–14.
- [11] B Aruna Kumari and K Vaisakh. 2022. Ensuring expected security cost with flexible resources using modified DE algorithm based dynamic optimal power flow. *Applied Soft Computing* 124 (2022), 108991.
- [12] Jane-Jing Liang, Boyang Qu, D Gong, and Cai Yue. 2019. Problem definitions and evaluation criteria for the CEC 2019 special session on multimodal multiobjective optimization. *Computational Intelligence Laboratory, Zhengzhou University* (2019), 353–370.
- [13] Tianyu Liu, Licheng Jiao, Wenping Ma, Jingjing Ma, and Ronghua Shang. 2016. A new quantum-behaved particle swarm optimization based on cultural evolution mechanism for multiobjective problems. *Knowledge-Based Systems* 101 (2016), 90–99.
- [14] Yang Lu and Jiaxian Yang. 2024. Quantum financing system: A survey on quantum algorithms, potential scenarios and open research issues. *Journal of Industrial Information Integration* 41 (2024), 100663.
- [15] Shunlong Luo. 2008. Quantum discord for two-qubit systems. *Physical Review A—Atomic, Molecular, and Optical Physics* 77, 4 (2008), 042303.
- [16] Harry Markowitz. 1952. Modern portfolio theory. *Journal of Finance* 7, 11 (1952), 77–91.
- [17] Francesco Menoncin. 2002. Optimal portfolio and background risk: an exact and an approximated solution. *Insurance: Mathematics and Economics* 31, 2 (2002), 249–265.
- [18] Ali Wagdy Mohamed, Anas A Hadi, Ali K Mohamed, Prachi Agrawal, Abhishek Kumar, and PN Suganthan. 2020. Problem definitions and evaluation criteria for the CEC 2021 special session and competition on single objective bound constrained numerical optimization. *Tech. Rep.* (2020).
- [19] Raymond Ros and Nikolaus Hansen. 2008. A simple modification in CMA-ES achieving linear time and space complexity. In *International conference on parallel problem solving from nature*. Springer, 296–305.
- [20] Justus Shunza, Mary Akinyemi, and Chika Yinka-Banjo. 2023. Application of quantum computing in discrete portfolio optimization. *Journal of Management Science and Engineering* 8, 4 (2023), 453–464.
- [21] Arvind R Singh, M. Wasim Abbas Ashraf, Davanam Ganesh, Rajkumar Singh Rathore, Chaminda T. E. R. Hewage, and Ali Kashif Bashir. 2025. Quantum-Inspired Metaheuristic Algorithms for Trust-Based Privacy Agreements and Secure Access in the Internet of Vehicles. *IEEE Transactions on Intelligent Transportation Systems* (2025), 1–13. doi:10.1109/TITS.2025.3591936
- [22] Lulu Song, Yun Dong, Qingxin Guo, Ying Meng, and Guodong Zhao. 2023. An adaptive differential evolution algorithm with DBSCAN for the integrated slab allocation problem in steel industry. *Applied Soft Computing* 146 (2023), 110665.
- [23] Shuangbao Song, Xingqian Chen, Yanxin Zhang, Zheng Tang, and Yuki Todo. 2021. Protein-ligand docking using differential evolution with an adaptive mechanism. *Knowledge-Based Systems* 231 (2021), 107433.
- [24] Andreas Tsanakas. 2008. Risk measurement in the presence of background risk. *Insurance: Mathematics and Economics* 42, 2 (2008), 520–528.
- [25] Jie Wei, Yuhui Zhang, and Wenhong Wei. 2025. HSEPSO: A hierarchical self-evolutionary PSO approach for UAV path planning. In *Proceedings of the Genetic and Evolutionary Computation Conference*. 1577–1584.
- [26] Sheng Xin Zhang, Yu Hong Liu, Xin Rou Hu, Jun Ting Luo, Li Ming Zheng, and Shao Yong Zheng. 2026. Differential evolution with dimensionally adaptive inheritance. *Engineering Applications of Artificial Intelligence* 163 (2026), 112587. doi:10.1016/j.engappai.2025.112587
- [27] Rui Zhong, Abdelazim G. Hussien, Shilong Zhang, Yuefeng Xu, and Jun Yu. 2025. Space mission trajectory optimization via competitive differential evolution with independent success history adaptation. *Applied Soft Computing* 171 (2025), 112777. doi:10.1016/j.asoc.2025.112777
- [28] Fang Zhu, Guoshuai Li, Hao Tang, Yingbo Li, Xvmeng Lv, and Xi Wang. 2024. Dung beetle optimization algorithm based on quantum computing and multi-strategy fusion for solving engineering problems. *Expert Systems with Applications* 236 (2024), 121219.

A Experimental detail

A.1 Quantitative evaluation

Due to space limitations, more data (including average values, standard deviations, Friedman mean ranks, and other details) are provided in this appendix. Tables 1–3 summarize the average values (Ave) and standard deviations (Std) for each algorithm, with QHDE's advantages highlighted through statistical analysis. Performance metrics include the W|T|L indicators in the first row, representing the number of functions where the algorithm achieved the best results (Win), tied (Tie), or the worst (Loss). The second row presents the Friedman mean, and the third row provides the overall ranking based on the Friedman test. The best results are shown in bold.

A.2 Portfolio selection

The main text only presents the convergence curves for 20 stocks. To provide a more complete overview, this appendix includes the convergence details for 40 to 80 stocks, offering a comprehensive illustration of QHDE's performance across different problem scales.

Table 1: Comparison of results on CEC 2020 (Dim=10).

ID	Metric	SASS	COLSHADE	sCMAES	HSEPSO	NDSOT	DE	ADE	QHDE
CEC2020-F1	Ave	1.2596E+02	1.5401E+05	4.7952E+04	1.5419E+03	9.0455E+08	8.7162E+03	2.1634E+04	8.3896E+03
	Std	3.2244E+01	2.6133E+05	8.6284E+03	2.0273E+03	8.0411E+08	6.2257E+03	2.0179E+04	3.4959E+03
CEC2020-F2	Ave	1.9527E+03	1.8713E+03	1.1608E+03	1.7670E+03	2.0611E+03	1.6134E+03	1.7921E+03	1.6346E+03
	Std	2.2923E+02	1.6680E+02	7.2102E+01	2.7436E+02	2.4009E+02	1.4799E+02	1.2385E+02	1.2887E+02
CEC2020-F3	Ave	1.0719E+03	7.2575E+02	7.1595E+02	7.3016E+02	7.5812E+02	7.2486E+02	7.3023E+02	7.2400E+02
	Std	8.9883E+01	3.9222E+00	1.7852E+00	9.8279E+00	1.5242E+01	2.2944E+00	4.0790E+00	1.8415E+00
CEC2020-F4	Ave	3.0867E+03	1.9018E+03	1.9014E+03	1.9013E+03	2.1379E+03	1.9020E+03	1.9026E+03	1.9016E+03
	Std	8.9578E+02	1.0413E+00	2.6121E-01	6.9844E-01	3.8232E+02	2.7200E-01	5.2237E-01	2.5906E-01
CEC2020-F5	Ave	5.0675E+05	2.8391E+03	1.3238E+05	5.6548E+03	3.2166E+04	9.3904E+04	5.3497E+04	1.5433E+04
	Std	3.4199E+05	1.0956E+03	1.5116E+05	4.3581E+03	3.6337E+04	5.3507E+04	4.6504E+04	1.0986E+04
CEC2020-F6	Ave	1.6329E+03	1.6009E+03	1.6671E+03	1.6076E+03	1.6056E+03	1.6008E+03	1.6009E+03	1.6006E+03
	Std	3.7445E+01	3.9231E-01	6.4484E+01	8.6316E+00	8.3936E+00	1.9871E-01	2.2818E-01	1.1185E-01
CEC2020-F7	Ave	1.4608E+05	2.3362E+03	9.5954E+03	4.2682E+03	3.5777E+05	1.6470E+04	1.3820E+04	3.1413E+03
	Std	1.1663E+05	3.4487E+02	3.6989E+03	2.8913E+03	1.1183E+06	1.5725E+04	7.4483E+03	6.7539E+02
CEC2020-F8	Ave	3.0374E+03	2.3015E+03	2.3981E+03	2.3026E+03	2.4664E+03	2.2968E+03	2.3032E+03	2.2806E+03
	Std	3.1887E+02	9.3281E-01	1.6992E+02	1.5297E+00	2.2345E+02	1.3396E+01	5.4518E-01	3.5335E+01
CEC2020-F9	Ave	2.5984E+03	2.6980E+03	2.7051E+03	2.7215E+03	2.7517E+03	2.7065E+03	2.7550E+03	2.7396E+03
	Std	4.3450E+01	8.8979E+01	5.4974E+01	7.9144E+01	1.0962E+02	4.9588E+01	4.0793E+00	2.0592E+01
CEC2020-F10	Ave	2.6971E+03	2.9182E+03	2.9403E+03	2.9126E+03	2.9449E+03	2.9127E+03	2.9317E+03	2.9031E+03
	Std	8.2033E+01	2.2016E+01	1.4788E+01	2.2074E+01	2.7204E+01	9.3948E+00	1.6121E+01	9.2580E+00
(W T L)		(3 3 4)	(2 8 0)	(2 7 1)	(1 9 0)	(0 6 4)	(0 10 0)	(0 9 1)	(2 8 0)
Friedman average		5.7	3.6	4.3	3.6	6.1	4.2	5.4	3.2
Overall Rank		7	2.5	5	2.5	8	4	6	1

Table 2: Comparison of results on CEC 2022 (Dim=10).

ID	Metric	SASS	COLSHADE	sCMAES	HSEPSO	NDSOT	DE	ADE	QHDE
CEC2022-F1	Ave	2.3556E+04	4.2548E+02	3.4512E+03	3.0000E+02	1.7145E+04	7.2421E+03	5.6459E+03	2.8877E+03
	Std	8.6503E+03	7.7959E+01	1.1366E+03	8.1732E-04	1.5821E+04	2.2748E+03	2.0879E+03	3.8819E+02
CEC2022-F2	Ave	4.0005E+02	4.0687E+02	4.0822E+02	4.0272E+02	4.6905E+02	4.0888E+02	4.0805E+02	4.0767E+02
	Std	4.8884E-02	9.5337E+00	1.4819E+00	4.2740E+00	5.9473E+01	5.2683E-01	7.9128E-01	9.6015E-01
CEC2022-F3	Ave	6.4866E+02	6.0002E+02	6.0017E+02	6.0163E+02	6.3036E+02	6.0000E+02	6.0000E+02	6.0000E+02
	Std	5.6665E+00	4.7401E-02	1.6434E-02	3.3538E+00	1.3205E+01	4.0309E-06	3.0085E-05	3.0682E-09
CEC2022-F4	Ave	8.4398E+02	8.1190E+02	8.0451E+02	8.2828E+02	8.3766E+02	8.2459E+02	8.2750E+02	8.1898E+02
	Std	1.0144E+01	3.8964E+00	1.8436E+00	1.1169E+01	1.0136E+01	4.6446E+00	4.1495E+00	4.8332E+00
CEC2022-F5	Ave	1.8979E+03	9.0003E+02	9.0002E+02	9.0473E+02	1.8269E+03	9.1538E+02	9.0056E+02	9.0002E+02
	Std	1.3630E+02	4.0493E-02	4.8295E-03	7.4980E+00	4.1216E+02	1.0397E+01	5.4330E-01	2.0449E-02
CEC2022-F6	Ave	2.1534E+03	1.9461E+03	8.2768E+03	3.4018E+03	4.5840E+03	5.4080E+03	7.5404E+03	6.0354E+03
	Std	3.1877E+02	1.7644E+02	2.5928E+03	1.7324E+03	1.6984E+03	3.2436E+03	3.9761E+03	1.7374E+03
CEC2022-F7	Ave	2.1079E+03	2.0206E+03	2.1069E+03	2.0332E+03	2.0806E+03	2.0059E+03	2.0144E+03	2.0047E+03
	Std	2.8718E+01	5.6505E+00	5.9625E+01	1.2532E+01	3.5487E+01	1.6793E+00	6.9743E+00	1.5625E+00
CEC2022-F8	Ave	2.2925E+03	2.2228E+03	2.2537E+03	2.2289E+03	2.2526E+03	2.2154E+03	2.2202E+03	2.2191E+03
	Std	9.3490E+01	3.6821E+00	5.0994E+01	3.9795E+01	3.7305E+01	4.6648E+00	5.7052E+00	4.7731E+00
CEC2022-F9	Ave	2.4629E+03	2.5331E+03	2.5293E+03	2.5293E+03	2.5821E+03	2.5293E+03	2.5293E+03	2.5293E+03
	Std	8.6355E+01	8.2581E+00	1.1728E-02	3.7130E-13	5.7991E+01	1.8473E-02	5.6655E-08	0.0000E+00
CEC2022-F10	Ave	2.7909E+03	2.5230E+03	2.5544E+03	2.6329E+03	2.7531E+03	2.4894E+03	2.4810E+03	2.5004E+03
	Std	1.6866E+02	4.7345E+01	1.2193E+02	1.4966E+02	4.2820E+02	1.6162E+01	4.1692E+01	3.7016E-02
CEC2022-F11	Ave	2.8437E+03	2.7074E+03	2.9034E+03	2.7150E+03	2.9042E+03	2.7441E+03	2.6743E+03	2.6301E+03
	Std	1.4825E+02	5.9401E+01	4.7247E-01	1.5996E+02	2.4626E+02	1.0915E+01	7.4199E+01	6.3423E+01
CEC2022-F12	Ave	2.9676E+03	2.8664E+03	2.8649E+03	2.8697E+03	2.8890E+03	2.8643E+03	2.8623E+03	2.8611E+03
	Std	3.6184E+01	2.3805E+00	5.0172E-01	1.0056E+01	2.6022E+01	1.3002E+00	1.0961E+00	1.2632E+00
(W T L)		(2 3 7)	(1 11 0)	(1 9 2)	(1 11 0)	(0 9 3)	(2 10 0)	(0 12 0)	(5 7 0)
Friedman average		6.33	4.36	5.06	6.52	3.77	3.47	4.25	2.24
Overall Rank		7	5	6	8	3	2	4	1

Table 3: Comparison of results on CEC 2022 (Dim=20).

ID	Metric	SASS	COLSHADE	sCMAES	HSEPSO	NDSOT	DE	ADE	QHDE
CEC2022-F1	Ave	7.5868E+04	5.5118E+03	4.5801E+04	3.0356E+02	7.2120E+04	3.6568E+04	4.6040E+04	2.4424E+04
	Std	1.0598E+04	1.5134E+03	8.2365E+03	5.3014E+00	1.9943E+04	6.2722E+03	9.2069E+03	6.1450E+03
CEC2022-F2	Ave	4.4526E+02	5.3263E+02	4.4958E+02	4.6389E+02	7.4214E+02	4.5393E+02	4.4858E+02	4.4911E+02
	Std	3.0707E+01	7.3684E+01	1.1313E-01	1.4303E+01	2.1824E+02	3.6461E+00	1.2496E+00	5.3291E-02
CEC2022-F3	Ave	6.6403E+02	6.0328E+02	6.0183E+02	6.0152E+02	6.6076E+02	6.0002E+02	6.0008E+02	6.0000E+02
	Std	7.1908E+00	3.7730E+00	1.5657E-01	9.5229E-01	1.5179E+01	5.3306E-03	4.9293E-02	6.4963E-04
CEC2022-F4	Ave	9.2314E+02	8.7471E+02	8.3482E+02	8.5850E+02	9.3188E+02	9.1870E+02	9.1756E+02	8.9373E+02
	Std	2.3613E+01	8.8732E+00	5.4823E+00	1.6713E+01	2.4614E+01	8.9196E+00	7.3839E+00	1.1874E+01
CEC2022-F5	Ave	3.8330E+03	9.7716E+02	9.0253E+02	1.4773E+03	4.2628E+03	1.8507E+03	1.1256E+03	9.4154E+02
	Std	1.6019E+02	5.1192E+01	5.6534E-01	4.7337E+02	6.3737E+02	3.6344E+02	1.3570E+02	1.2793E+01
CEC2022-F6	Ave	1.9286E+03	3.1497E+03	2.5138E+06	4.6641E+03	3.3872E+05	2.0281E+06	2.7157E+06	9.3384E+05
	Std	5.8741E+01	1.4007E+03	7.4608E+05	3.1005E+03	7.0089E+05	8.8171E+05	2.0340E+06	8.9280E+05
CEC2022-F7	Ave	2.2320E+03	2.0825E+03	2.0888E+03	2.1300E+03	2.2013E+03	2.0541E+03	2.0638E+03	2.0402E+03
	Std	6.7248E+01	1.5553E+01	1.2713E+01	5.5673E+01	7.9075E+01	1.0546E+01	1.3387E+01	4.5202E+00
CEC2022-F8	Ave	2.5956E+03	2.2322E+03	2.2416E+03	2.2493E+03	2.2792E+03	2.2282E+03	2.2316E+03	2.2268E+03
	Std	2.1015E+02	2.8707E+00	7.5597E+00	4.9364E+01	6.0005E+01	1.1707E+00	1.4037E+00	9.0278E-01
CEC2022-F9	Ave	2.4272E+03	2.4967E+03	2.4829E+03	2.4808E+03	2.6969E+03	2.4809E+03	2.4808E+03	2.4808E+03
	Std	4.0977E+01	9.4419E+00	7.9000E-01	5.3717E-02	1.5256E+02	9.7530E-02	1.9382E-02	6.2833E-04
CEC2022-F10	Ave	4.3504E+03	2.5166E+03	3.2527E+03	3.0804E+03	4.8266E+03	2.5150E+03	2.5676E+03	2.5074E+03
	Std	1.7332E+02	4.9908E+01	3.1930E+02	4.3315E+02	6.1308E+02	8.8013E+00	8.5423E+01	1.2622E+01
CEC2022-F11	Ave	3.0203E+03	3.2229E+03	2.9762E+03	2.8804E+03	4.3933E+03	2.9255E+03	2.9010E+03	2.9414E+03
	Std	3.3857E+02	8.9757E+01	8.4273E+00	1.0354E+02	7.2732E+02	2.8293E+01	2.0670E+00	1.3077E+02
CEC2022-F12	Ave	3.6308E+03	2.9913E+03	2.9526E+03	2.9903E+03	3.0752E+03	2.9501E+03	2.9466E+03	2.9442E+03
	Std	2.0543E+02	2.9376E+01	1.5824E+01	2.7236E+01	8.9021E+01	2.2490E+00	4.2949E+00	5.9966E+00
(W T L)		(1 7 4)	(1 11 0)	(2 10 0)	(1 11 0)	(0 5 7)	(0 12 0)	(0 11 1)	(7 5 0)
Friedman average		5.9	4.34	4.45	3.80	7.11	4.15	3.87	2.35
Overall Rank		7	5	6	2	8	4	3	1

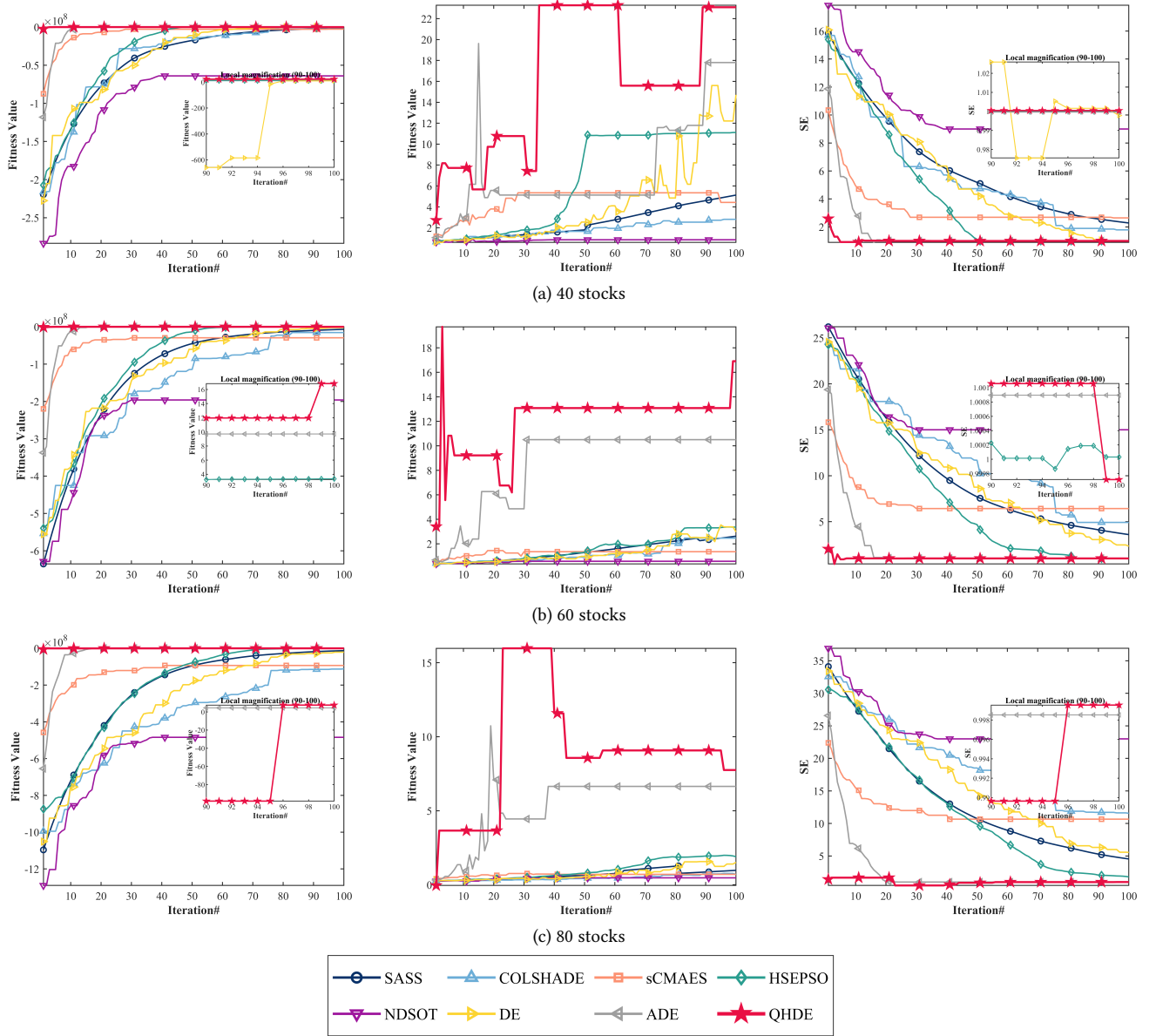


Figure 1: Evaluation and comparison of QHDE applied to 40-80 stocks alongside other metaheuristic algorithms.